



Article

Hydroplumboelsmoreite, $(\text{Pb}_1\Box_1)_{\Sigma 2}(\text{W}_{1.33}\text{Fe}_{0.67}^{3+})_{\Sigma 2}\text{O}_6(\text{H}_2\text{O})$, a redefined mineral species of the elsmoreite group from China

Xue Yuan^{1,2} , Sun Ningyue¹, Li Guowu^{1*} and Yang Guangming³

¹Crystal Structure Laboratory, Science Research Institution, China University of Geosciences (Beijing), 100083 Beijing, China; ²School of Materials Science and Technology, China University of Geosciences (Beijing), 100083 Beijing, China; and ³State Key Laboratory of Geological Process and Mineral Resources, China University of Geosciences, Wuhan 430074, China

Abstract

Hydroplumboelsmoreite (IMA21-C), $(\text{Pb},\Box)_2(\text{W},\text{Fe}^{3+})_2\text{O}_6(\text{H}_2\text{O})$, is a redefined elsmoreite-group mineral in the pyrochlore supergroup. It was found in a ‘jixianite’ cotype specimen provided by Mr. Liu Jianchang, who first found ‘jixianite’ in 1979 in the Jizhou District, Tianjin City, China. The mineral occurs as yellow to reddish brown aggregates, together with raspite and another elsmoreite-group mineral under study. Hydroplumboelsmoreite occurs in cryptocrystalline form and occasionally in octahedral microcrystalline form (under 20 μm in size). The crystals are colourless and translucent with a white streak, and the lustre is adamantine to greasy. Hydroplumboelsmoreite is isotropic, with a calculated refractive index of 2.29, a Mohs hardness of $\sim 4\frac{1}{2}$ –5, and a calculated density of 7.47 $\text{g}\cdot\text{cm}^{-3}$. The strongest five powder X-ray diffraction lines [d in $\text{\AA}(I)(hkl)$] are 6.070(28)(111), 3.012(100)(222), 2.603(32)(004), 1.836(35)(044) and 1.568(30)(226). The crystal structure was refined to $R_1 = 0.0459$ using 80 unique reflections collected with $\text{MoK}\alpha$ radiation, and the results show that the mineral is cubic, space group $Fd\bar{3}m$, with $a = 10.3377(5)$ \AA , $V = 1104.77(16)$ \AA^3 and $Z = 8$. Electron microprobe analyses and crystal structure refinement were used to determine the empirical formula: $(\text{Pb}_{1.05}\text{Sr}_{0.05}\text{Ce}_{0.07}^{3+}\text{Na}_{0.01}\Box_{0.82})_{\Sigma 2.00}(\text{W}_{1.32}\text{Fe}_{0.67}^{3+}\text{Zr}_{0.01})_{\Sigma 2.00}\text{O}_6[(\text{H}_2\text{O})_{0.43}\text{O}_{0.19}\Box_{0.38}]_{\Sigma 1.00}$. The mineral was named hydroplumboelsmoreite based on the predominance of Pb, W, and molecular H_2O in the A, B and Y sites, respectively.

Keywords: hydroplumboelsmoreite, elsmoreite, pyrochlore supergroup, crystal structure, tungsten

(Received 2 August 2021; accepted 13 November 2021; Accepted Manuscript published online: 3 December 2021; Associate Editor: Michael Rumsey)

Introduction

‘Jixianite’ used to be an approved mineral found in the Yanhe tungsten deposit in Jixian County, Hebei (currently Jizhou District in Tianjin City), China, by Liu (1979). It was an oxide containing W and Pb components and was approved by the International Mineralogical Association Commission on New Minerals and Mineral Names (IMA–CNMNC) at that time. However, because of the mineral’s tiny crystal size, the single crystal structure data could not be obtained. According to the powder-diffraction data, the diffraction characteristics are similar to those of pyrochlore-super group minerals, so it was classified as a pyrochlore-group mineral containing W and Pb, with the formula $\text{Pb}_2(\text{W},\text{Fe})_2(\text{O},\text{OH})_7$.

The general formula for the pyrochlore supergroup is $A_{2-m}B_2X_{6-w}Y_{1-n}$ (Atencio *et al.*, 2010). In 2010, based on the proposed new scheme for the nomenclature of the pyrochlore supergroup, which was approved by the IMA–CNMNC, ‘jixianite’ was discredited due to the absence of a detailed crystal structure study and lack of information about the Y site dominant anion (Atencio

et al., 2010). More recently, the status of the mineral’s name has been changed from ‘discredited’ to ‘questionable’ pending further research (Christy and Atencio, 2013).

Recently, we obtained a cotype specimen from Mr. Liu Jianchang who first found ‘jixianite’ in 1979 and we also collected new samples from the type locality. We selected 156 fragments from the cotype specimen to make an epoxy block for single-side polishing, including the residual part of the fragment used for structural data collection. Infrared spectroscopy, Raman spectroscopy and electron microprobe analysis were all performed on the polished surface of this sample group. Through this investigation, we discovered two members of the elsmoreite group within the pyrochlore supergroup in the cotype specimen of ‘jixianite’, including hydroplumboelsmoreite (IMA21-C, Miyawaki, 2021), which replaces ‘jixianite’, and a potential new mineral provisionally named ‘hydroelsmoreite’ (IMA2019-066, pending resubmission).

In this study, a 1.2 kW high-power microfocus rotating anode X-ray source and a hybrid pixel array detector single-crystal diffractometer were used to analyse the structure, and the single-crystal diffraction data were obtained for a small crystal (10 $\mu\text{m} \times 10 \mu\text{m} \times 10 \mu\text{m}$ in size). The results show that hydroplumboelsmoreite crystallises in the cubic system, space group $Fd\bar{3}m$, with lattice parameters of $a = 10.3377(5)$ \AA , $V = 1104.77(16)$ \AA^3 and $Z = 8$, so it has a pyrochlore type structure.

*Author for correspondence: Li Guowu, Email: liguowu@cugb.edu.cn

Cite this article: Yuan X., Ningyue S., Guowu L. and Guangming Y. (2021) Hydroplumboelsmoreite, $(\text{Pb}_1\Box_1)_{\Sigma 2}(\text{W}_{1.33}\text{Fe}_{0.67}^{3+})_{\Sigma 2}\text{O}_6(\text{H}_2\text{O})$, a redefined mineral species of the elsmoreite group from China. *Mineralogical Magazine* 85, 890–900. <https://doi.org/10.1180/mgm.2021.86>

© The Author(s), 2021. Published by Cambridge University Press on behalf of The Mineralogical Society of Great Britain and Ireland. This is an Open Access article, distributed under the terms of the Creative Commons Attribution licence (<http://creativecommons.org/licenses/by/4.0/>), which permits unrestricted re-use, distribution and reproduction, provided the original article is properly cited.

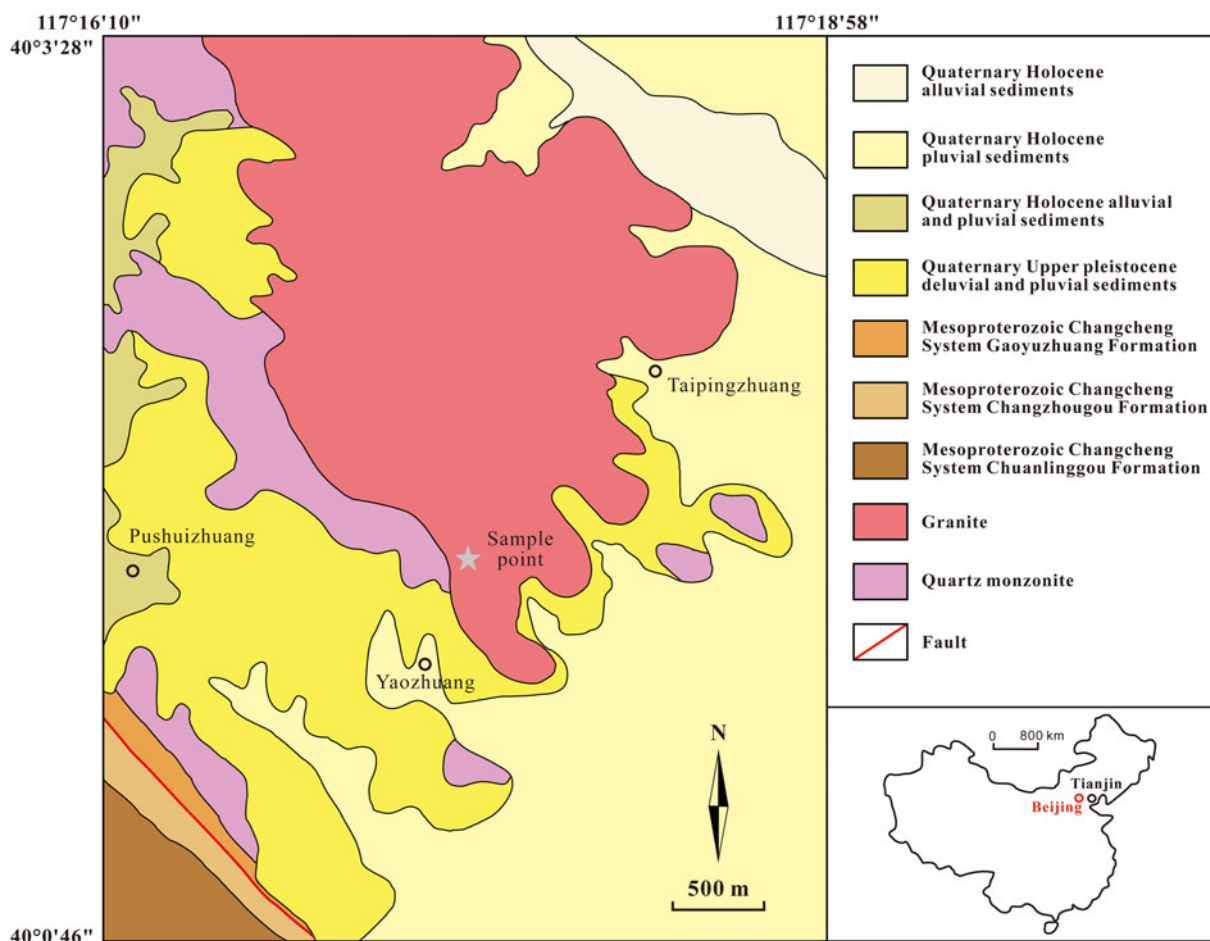


Fig. 1. Geological map of the locality.

The new electron-microprobe analyses carried out on hydroplumboelsmoreite are more accurate than the previous analyses, and were used to determine a simplified formula: $(\text{Pb}, \square)_2(\text{W}, \text{Fe}^{3+})_2\text{O}_6(\text{H}_2\text{O})$. According to the nomenclature of the pyrochlore supergroup, the mineral 'jixianite' is redefined as hydroplumboelsmoreite as it corresponds to a member of the elsmoreite group with Pb dominant in the A site and H_2O dominant in the Y site.

Hydroplumboelsmoreite and its name have been approved by the IMA–CNMNC and replaces 'jixianite'. The type specimen of hydroplumboelsmoreite has been registered within the collections of the Geological Museum of China (Xisi Yangrou hutong No. 15, Xicheng District, Beijing), China, under catalogue number M16125.

Occurrence and paragenesis

The mineral was discovered in the oxidised section of hydrothermal tungsten-bearing lead deposits in the Yanhe tungsten deposit in Jixian County, Hebei Province, China, which is now called the Jizhou District in Tianjin City (40°1'54.8"N, 117°17'22.4"E).

The Jixian Yanhe tungsten deposit is situated in the middle of the Yanshan subsidence belt, the west wing of the Malanyu anticline, the southwest section of the Panshan short-axis anticline, and the southern border of the contact zone of the Panshan rock body (porphyritic quartz monzonite) (Fig. 1). The deposit is a high-temperature hydrothermal tungsten-bearing quartz vein type

deposit (Wang *et al.*, 2013). The tungsten mineralisation was related closely to magmatic activity and occurs in the inner contact zone of the rock. The metallogenic rock is mainly Late Indosinian intermediate-felsic rock, and the ore-bearing surrounding rocks are quartz monzonite and medium-to-fine-grained granite (Wen *et al.*, 2015). The occurrence, morphology, and scale of the tungsten-bearing quartz veins are strictly controlled by the lithology and structural fractures (Wen *et al.*, 2015). More than 290 quartz veins have been found in this area (Wang *et al.*, 2013).

Hydroplumboelsmoreite occurs in the oxidised section of the tungsten-bearing quartz veins (Liu, 1979). The primary minerals in the oxidised zone include quartz, pyrite, ferberite, cassiterite, chalcopyrite, scheelite, acanthite, silver and copper. The secondary minerals found nearby mainly include muscovite, bismutite, raspite, wulfenite, malachite, covellite, hydroplumboelsmoreite, and 'hydroelsmoreite' (under investigation).

Hydroplumboelsmoreite is an uncommon secondary mineral formed in the oxidised zone of the hydrothermal tungsten-bearing lead deposits. It mostly occurs as microcrystalline to cryptocrystalline aggregates, with an earthy, honeycombed, or crusty appearance (Fig. 2a), and the single crystals are tiny (Fig. 2b), exhibiting the characteristics of a hypergene mineral. The mineral is commonly intergrown with raspite (Fig. 2c,d) and 'hydroelsmoreite', and may be formed as a secondary mineral after scheelite, ferberite and wulfenite.

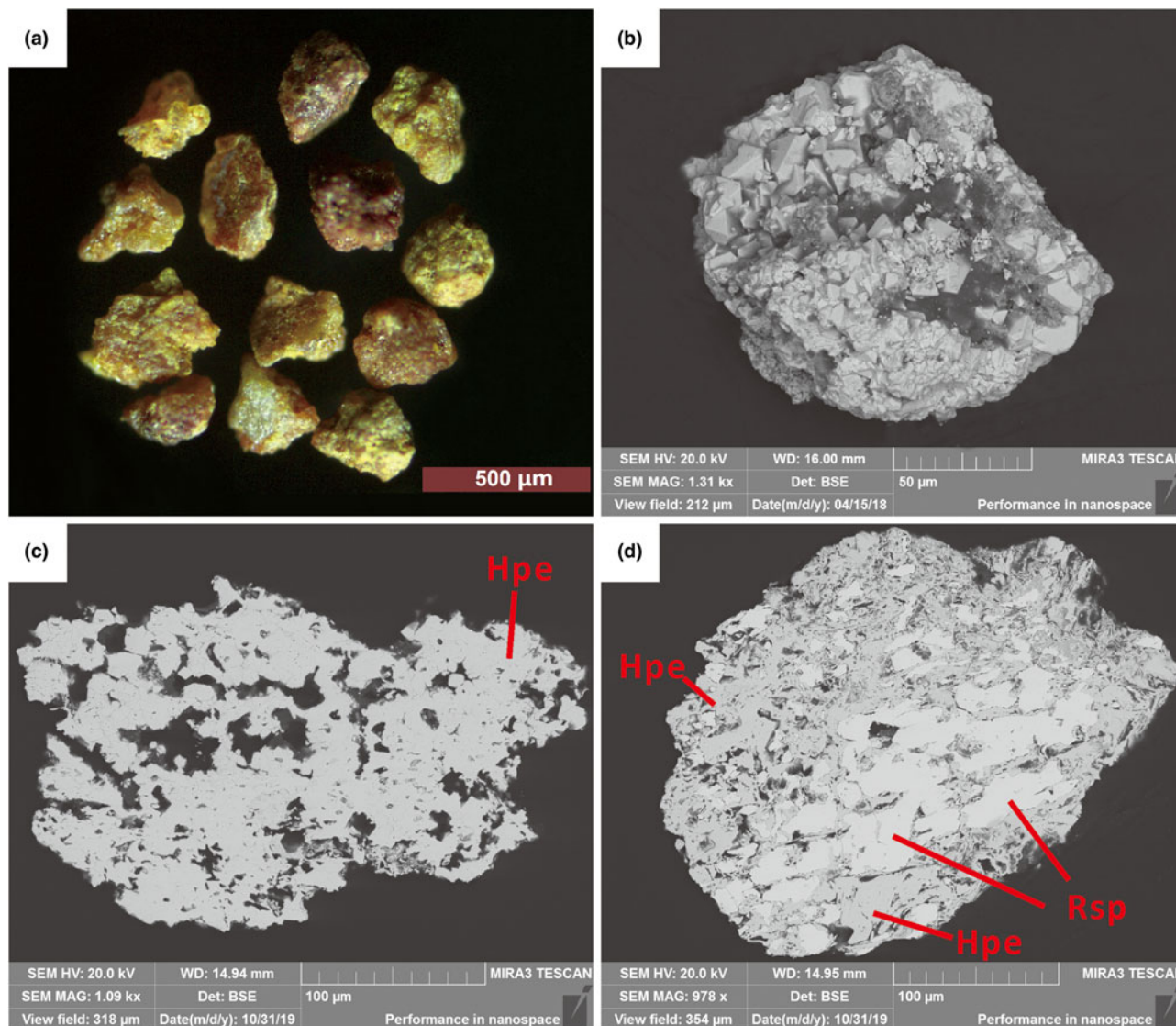


Fig. 2. Aggregate grains of hydroplumboelsmoreite: (a–c) aggregate grains of hydroplumboelsmoreite (Hpe) and (d) paragenetic raspite (Rsp) (symbols according to Warr, 2021).

Appearance and physical and optical properties

Generally, the aggregations reach 300 µm in size, but crystals are <20 µm across (Fig. 2a,b). Monocrystals are rare, and they are sub-hedral or allotriomorphic granular, with the dominant form {111}. The aggregates are yellow or reddish brown (Fig. 2a). The crystals are colourless with a white streak, translucent with a greasy lustre, brittle with a conchoidal fracture, and no apparent twinning, cleavage, or parting was observed.

Hydroplumboelsmoreite is isotropic, and the refractive index calculated based on its chemical composition and Gladstone–Dale relationship ($N = K_d + 1$, K from Mandarino, 1981) is 2.29. No fluorescence was observed.

The density could not be measured because the single-crystal particles of this mineral are tiny and are generally intergrown with other minerals. However, the density calculated based on the empirical formula and the unit cell parameters refined from the single-crystal X-ray diffraction data is 7.47 g·cm⁻³. Vickers microhardness tests generally gave values of 278.59–302.3 kg·mm⁻² (HV0.1kgf), and the Mohs hardness estimated by the VHN test is ~4½–5.

Spectroscopy

Infrared spectrum

The infrared (IR) spectrum of a polished surface of hydroplumboelsmoreite was obtained using a Bruker27 IR microscope equipped with a liquid nitrogen-cooled detector in reflection mode. The spectrum in the range of 4000–400 cm⁻¹ was collected by averaging 32 scans at a resolution of 4 cm⁻¹. The IR spectrum is shown in Fig. 3. The samples were stored at 110°C for 2 hours before the analysis to avoid the effect of adsorbed water on the test results. The 3552 cm⁻¹(strong) and 1631 cm⁻¹(medium) bands represent the stretching vibration and bending vibration of H₂O, respectively. The IR absorption related to the W=O stretching vibration is represented by two peaks at 916(weak) and 859(weak) (Gadsden, 1975; Farmer, 1982). All of the other bands in the 400–700 cm⁻¹ range are due to the vibrations of the elsmoreite-type framework.

Raman spectrum

The Raman spectrum was obtained using a RENISHAW in Via-Reflex microscope Raman spectrometer equipped with a

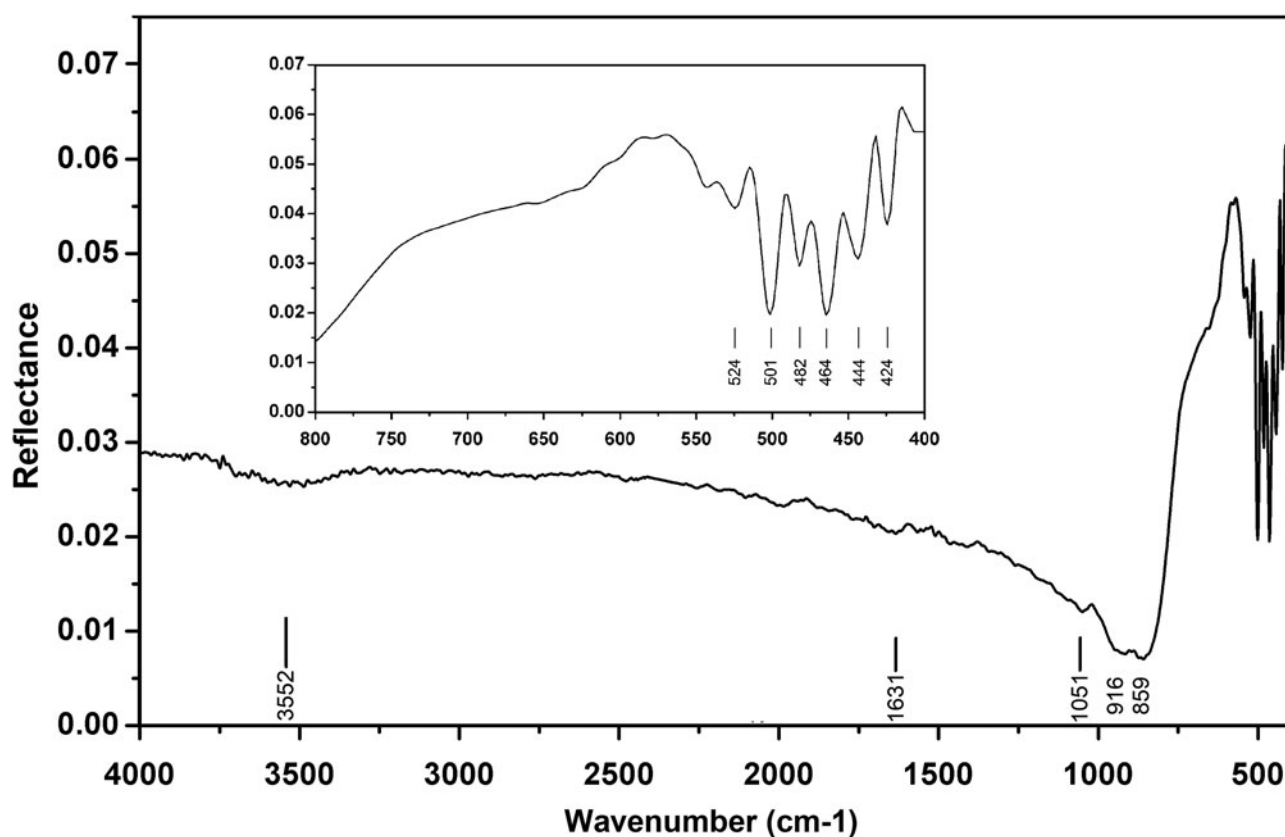


Fig. 3. Infrared spectrum of hydroplumboelsmoreite.

532 nm laser, in reflection mode, and the data acquisition time was 10 s. The Raman spectrum is shown in Fig. 4. The Raman spectrum of hydroplumboelsmoreite is characterised by an intense band at 891 cm⁻¹ (W=O stretching) (Mills *et al.*, 2017). The bands at 695 and 501 cm⁻¹ correspond to the O–W–O stretching modes, while the bands at 436 and 362 cm⁻¹ correspond to the O–W–O bending modes (Gu *et al.*, 2006). The bands in the 100–350 cm⁻¹ region are assigned to the lattice modes.

The band at 1583 cm⁻¹ is an indicator of molecular H₂O, which is consistent with the IR spectrum. There is no obvious O–H stretching vibration band between 3400 and 3500 cm⁻¹.

Chemical composition

An average of ten spot-analyses was obtained using an electron microprobe (JEOL JXA-8100, wavelength-dispersive spectrometry mode (WDS), 20 kV, 10 nA and 2 μm beam diameter). The analytical data for hydroplumboelsmoreite and ‘hydroelsmoreite’, and the reported data for ‘jixianite’ are summarised in Table 1. It was found that the contents and total amounts of the different components of hydroplumboelsmoreite and ‘hydroelsmoreite’ are significantly different while the hydroplumboelsmoreite data are rather similar to those for ‘jixianite’.

The samples were stored again, at 110°C for 2 hours before the compositional analysis to avoid the effect of adsorbed water on the test results. Due to the very small particle-size of the hydroplumboelsmoreite, direct determination of H₂O was not possible. The H₂O was calculated based on the structure refinement. The presence of molecular H₂O and the absence of OH groups were confirmed by the infrared (IR) and Raman spectra. The dominant

occupant of the Y site (O2) was H₂O, which is consistent with the structure refinement, the bond valence sum, and the chemical composition analysis.

Given the known occurrence of hydroplumboelsmoreite in the oxidised zone, the appearance of typical supergene characteristics, the low scattering factor for the W1 site based on the structure refinement, and based on previous studies of elsmoreite-group minerals, all of the Fe was assumed to be trivalent and was assigned to the B site. Ce, Sr, Na and Ca were assumed to be confined to the A site.

On the basis of the results from the electron microscope analyses and crystal structure refinement (see below), the empirical formula is (Pb_{1.05}Sr_{0.05}Ce_{0.07}Na_{0.01}□_{0.82})_{Σ2.00}(W_{1.32}Fe_{0.67}Zr_{0.01})_{Σ2.00}O₆[(H₂O)_{0.43}O_{0.19}□_{0.38}]_{Σ1.00}, calculated on the basis of B = 2.

Moreover, because hydroplumboelsmoreite and ‘hydroelsmoreite’ are indistinguishable in terms of appearance, it is not possible to determine whether the chemical data for ‘jixianite’ (Liu, 1979) derived via wet-chemical analysis using larger amounts of subsample are accurate or not, and we speculate that the sample analysed may have been a mixture of raspite, hydroplumboelsmoreite and ‘hydroelsmoreite’.

X-ray diffraction and crystallography

Powder X-ray diffraction

The powder X-ray diffraction data (Table 2) were obtained using a Rigaku Oxford Diffraction XtaLAB PRO-007HF (MoKα, 50 kV and 24 mA) by the powder rotations method, from the 0.2 mm × 0.2 mm × 0.2 mm aggregated fragment used for all

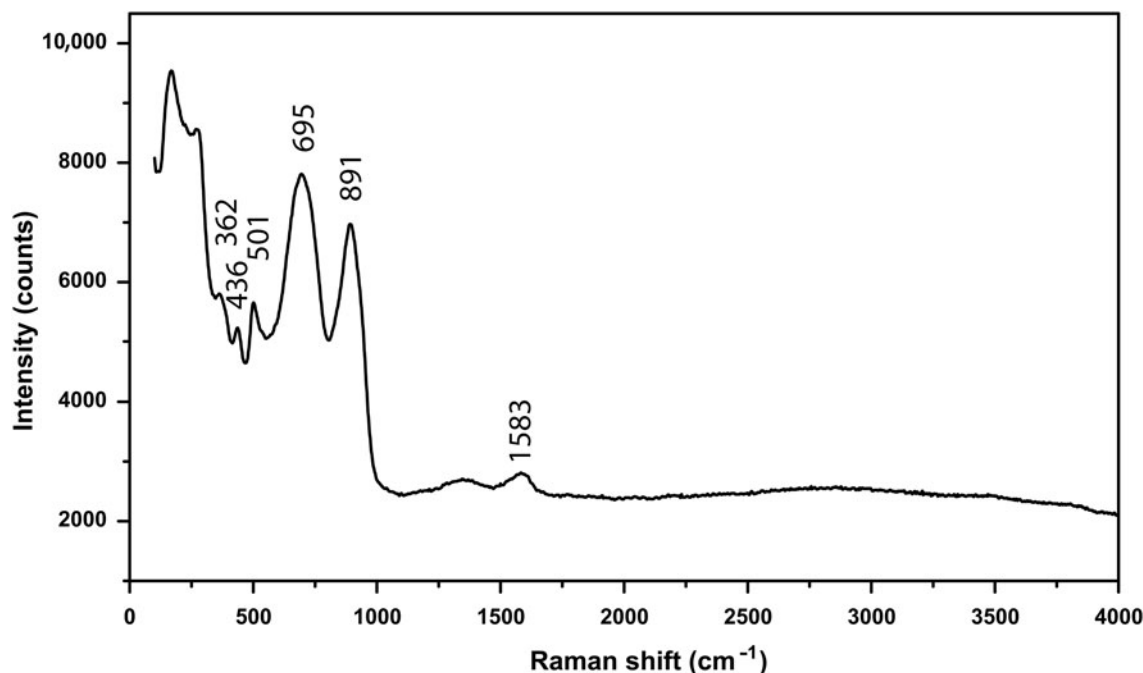


Fig. 4. Raman spectrum of hydroplumboelsmoreite.

Table 1. Chemical data (in wt.%) for hydroplumboelsmoreite, 'hydroelsmoreite' and 'jixianite'.

Constituent	Hydroplumboelsmoreite			'Hydroelsmoreite'			Probe standard	'Jixianite' **
	Mean	Range	S.D.	Mean	Range	S.D.		Mean
MgO	–	–	–	0.01	0–0.03	0.01	Pyrope	0.20
Na ₂ O	0.03	n.d.–0.12	0.04	0.27	0.05–0.38	0.09	Albite	–
WO ₃	48.71	46.23–51.33	1.69	59.82	52.72–63.23	3.22	Scheelite	50.39
PbO	37.49	35.27–40.40	1.66	22.70	19.77–27.49	2.23	PbCrO ₄	38.72
SrO	0.90	0.81–0.99	0.05	0.95	0.88–1.08	0.06	Celestite	–
Al ₂ O ₃	0.01	n.d.–0.04	0.01	0.20	0–0.75	0.30	Y ₃ Al ₅ O ₁₂	–
Fe ₂ O ₃	8.50	8.05–9.03	0.36	6.75	4.53–11.11	2.25	Synthetic Fe	7.24(FeO***)
K ₂ O	0.01	n.d.–0.04	0.01	0.04	0–0.11	0.03	Sanidine	–
MnO	0.01	n.d.–0.04	0.02	0.04	0–0.11	0.04	MnSiO ₃	–
CaO	0.04	n.d.–0.15	0.05	0.43	0.1–0.62	0.16	CaSiO ₃	–
Ta ₂ O ₅	0.03	n.d.–0.13	0.04	0.09	0–0.40	0.13	Manganotantalite	–
ZrO ₂	0.26	0.16–0.36	0.08	0.27	0.09–0.39	0.08	ZrO ₂	–
Ce ₂ O ₃	1.73	1.61–1.85	0.08	1.67	1.18–2.08	0.29	Monazite-(Ce)	–
Nb ₂ O ₅	0.06	n.d.–0.26	0.09	0.09	0–0.18	0.07	KNbO ₃	–
UO ₂	0.01	n.d.–0.06	0.02	–	–	–	Metallic uranium	–
F	n.d.	n.d.	n.d.	n.d.	n.d.	n.d.	Fluorapatite	–
TiO ₂	0.03	n.d.–0.08	0.04	–	–	–	Rutile	–
MoO	–	–	–	–	–	–	–	0.01
CuO	–	–	–	–	–	–	–	0.27
Total	97.81	97.16–98.56	0.43	93.34	92.11–94.50	0.79	–	96.83
H ₂ O*	1.27	–	–	–	–	–	–	–

Notes: 'hydroelsmoreite' and 'jixianite' are not valid minerals approved by the IMA (Pasero, 2021). S.D. = standard deviation; n.d. = not detected; '–' = not analysed

* H₂O calculated by structure refinement; **Data from Liu (1979); ***FeO = Fe₂O₃ + FeO

the test. The powder X-ray diffraction pattern of hydroplumboelsmoreite (MoK α) is shown in Fig. 5. The five strongest powder X-ray diffraction lines [d in Å(I)(hkl)] are 6.070(28)(111), 3.012(100)(222), 2.603(32)(004), 1.836(35)(044) and 1.568(30)(226). The unit cell parameters refined from the powder-diffraction data using the *Chexcell* software (Jean and Bernard, 2001) are as follows: cubic, $Fd\bar{3}m$ (#227), $a = 10.388(11)$ Å, $V = 1121(3)$ Å³ and $Z = 8$.

Single-crystal X-ray diffraction and structure determination

The single-crystal X-ray analysis was carried out using a Rigaku Oxford Diffraction XtaLAB PRO-007HF rotating anode micro-focus X-ray source (1.2 kW, MoK α , $\lambda = 0.71073$ Å) and a hybrid pixel array detector single-crystal diffractometer. The analytical conditions were 50 kV, 24 mA and an exposure time of 100 s per frame. A single crystal particle (10 $\mu\text{m} \times 10 \mu\text{m} \times 10 \mu\text{m}$ in

Table 2. Powder X-ray diffraction data (d in Å) for hydroplumboelsmoreite.

I_{obs}	I_{calc}	d_{obs}	d_{calc}	hkl
28	10	6.070	5.998	111
19	5	3.156	3.132	113
100	100	3.012	2.999	222
32	34	2.603	2.597	004
8	2	2.000	1.999	115
35	35	1.836	1.837	044
5	2	1.753	1.756	135
30	31	1.568	1.566	226
9	8	1.499	1.500	444
6	1	1.455	1.455	117
6	1	1.349	1.353	355
6	4	1.298	1.299	008
11	9	1.192	1.192	266
7	7	1.161	1.162	048

The strongest lines are given in bold.

size) from the powder X-ray diffraction sample was analysed. The structure solution and refinement were performed using *SHELX 2014* (Sheldrick, 2015), and the crystal structure was determined using the direct method. The details of the data collection and structure refinement for hydroplumboelsmoreite are summarised in Table 3. The atom coordinates and site occupancies are listed in Table 4. The anisotropic displacement parameters are listed in Table 5. Selected geometric parameters are listed in Table 6. The bond valences and bond-valence sums are presented in Table 7. The crystal structure of hydroplumboelsmoreite is shown in Fig. 6. The crystal structure refinement converged to $R_1 = 0.0459$ for 80 reflections with $|F_o| > 4\sigma F$ and 0.0509 for all 94 reflections. The crystallographic information file has been

deposited with the Principal Editor of *Mineralogical Magazine* and is available as Supplementary material (see below).

The research results show that this mineral crystallises in the cubic system, space group $Fd\bar{3}m$, with lattice parameters of $a = 10.3377(5)$ Å, $V = 1104.77(16)$ Å³ and $Z = 8$. The crystal structure is the pyrochlore type structure. W is [6]-coordinated (site 16c), is located at the centre of octahedron, and the W–O bond length is 1.944 Å. Pb, as a large cation, is [8]-coordinated (site 16d), is distributed in the channel, and the Pb–O bond length is 2.238 Å and 2.652 Å. Pb dominantly occupies the A site, while H₂O predominantly occupies the Y site (site 8b). Thus, hydroplumboelsmoreite is still a pyrochlore-supergrout mineral. The ideal end-member formula is $(\text{Pb}_1\Box_1)_{\Sigma 2}(\text{W}_{1.33}\text{Fe}_{0.67})_{\Sigma 2}\text{O}_6(\text{H}_2\text{O})$ based on the crystal structure.

The structure refinement process and water content analysis were as follows: The occupancy of the A and B sites were fixed based on the compositional data collected from the homologous particle. The A site was occupied predominantly by Pb; and the B site was occupied by W and Fe. As other members of the elsmoreite group, i.e. hydroxyknoelsmoreite (Mills *et al.*, 2017), are found in lower symmetric space groups due to the ordered distributions of Fe and W, we tried to find lower symmetric space groups to solve the structure of hydroplumboelsmoreite, however no satisfactory results were found. Hence, the W and Fe should be disordered in our sample. The B site was fixed with $(\text{W}_{1.33}\text{Fe}_{0.67}^{3+})$ in the refinement process. The X site was assumed to be fully occupied, which was proven by the bond valence sums (BVS).

When we assumed the Y site (O2) was fully occupied by O[#] (e.g. O²⁻, OH⁻, or H₂O), the U_{eq} of O2 was 0.14766 Å², which seemed too high for O atoms. This may have been due to the following two reasons: (1) the quality of the diffraction data was not

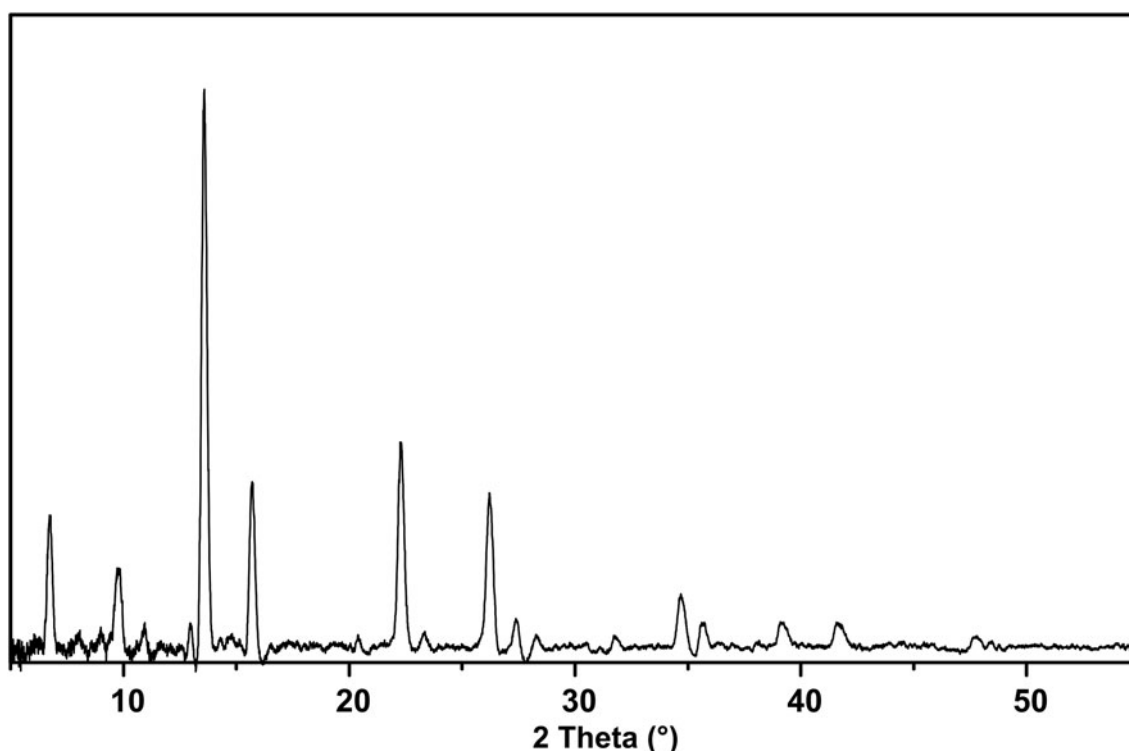


Fig. 5. Powder X-ray diffraction pattern of hydroplumboelsmoreite (MoK α).

Table 3. Data collection and structure refinement details for hydroplumboelsmoreite.

Crystal data	
Formula derived from the structure refinement	Pb _{1.01} (W _{1.33} Fe _{0.67}) _{Σ2} O ₆ (H ₂ O) _{0.62}
Crystal size (mm)	0.01 × 0.01 × 0.01
Temperature (K)	293(2)
<i>a</i> , <i>b</i> , <i>c</i> (Å)	10.3377(5), 10.3377(5), 10.3377(5)
α, β, γ (°)	90, 90, 90
<i>V</i> (Å ³)	1104.77(16)
<i>Z</i>	8
Calculated density (g·cm ⁻³)	7.382
μ (mm ⁻¹)	60.878
Data collection	
Crystal description	Colourless octahedral grain
Instrument	XtaLAB PRO-007HF
Radiation type, wavelength (Å)	MoKα, 0.71073
2θ range (°)	6.826 to 58.176
Absorption correction	Multi-scan
<i>T</i> _{min} , <i>T</i> _{max}	0.61312, 1.00000
No. of measured, independent and observed [<i>I</i> > 2σ(<i>I</i>)] reflections	1549, 94, 80
<i>R</i> _{int}	0.0509
Data completeness to 25.242°θ (%)	100
Indices range of <i>h</i> , <i>k</i> , <i>l</i>	-14 ≤ <i>h</i> ≤ 9, -14 ≤ <i>k</i> ≤ 12, -14 ≤ <i>l</i> ≤ 9
Refinement	
Refinement	Full-matrix least squares on <i>F</i> ²
Weighting coefficients <i>a</i> , <i>b</i> *	0.061, 39.6
Number of reflections, parameters, restraints	94, 11, 0
<i>R</i> ₁ [<i>I</i> > 2σ(<i>I</i>)], <i>R</i> ₁ (all)	0.0459, 0.0509
<i>wR</i> ₂ [<i>I</i> > 2σ(<i>I</i>)], <i>wR</i> ₂ (all)	0.1237, 0.1269
GoF	1.322
Δρ _{max} , Δρ _{min} (e ⁻ Å ⁻³)	1.86, -1.56

$$*w = 1/(\sigma^2(F_o^2) + (aP)^2 + bP), \text{ where } P = [\max(F_o^2, 0) + 2F_c^2]/3$$

Table 4. Atomic coordinates for hydroplumboelsmoreite.

Atom	Wyckoff	Occupancy	<i>x/a</i>	<i>y/b</i>	<i>z/c</i>
Pb1(≡A)	16c	0.504	¾	½	¼
W1(≡B)	16d	0.667	½	¼	¼
Fe1(≡B)	16d	0.333	½	¼	¼
O1(≡X)	48f	1	0.5641(10)	¾	¾
O2(≡Y)	8a	0.62(6)	¾	¾	½

satisfactory; and (2) the *Y* site was not fully occupied by O[#]. The first reason seems untenable, as there is another O1 atom (*X* site) in the structure with a lower *U*_{eq} value of 0.027, and the *R*₁ and *wR*₂ values are acceptable (Table 8). As for the second reason, in pyrochlore-supergroup minerals (including the elsmoreite group), the *Y* site can be occupied by □, O²⁻, OH⁻, H₂O, F⁻, K⁺, Cs⁺ and Rb⁺ (Atencio et al., 2010). The electron microprobe analysis (EMPA) data shows that there are trace amounts of K,

Table 6. Selected geometric bond distances (Å) for hydroplumboelsmoreite.

Pb1–O2	2.238(0) × 2	W1(Fe1)–O1	1.944(3) × 6
Pb1–O1	2.652(7) × 6	<W(Fe)–O>	1.944
<Pb–O>	2.549		

Table 7. Bond-valence sums for hydroplumboelsmoreite.

	<i>A</i> site	<i>B</i> site	O sum
O1	0.124×6↓ 0.124×2→	0.627×6+0.203×6↓	1.908
O2	0.180×2↓ 0.180×4→	0.627×2+0.203×2→	0.720
Sum	1.104	4.980	

Note: The bond strength for the *A* site is based on an occupancy of 0.504Pb²⁺, a *B* site occupancy of 0.667W⁶⁺ + 0.333Fe³⁺, and an O2 occupancy of 0.626. The bond-valence calculations were done using the equation and constants of Brown (1977), $S = \exp[R_0 - d_0]/b$, bond parameters for Pb²⁺–O from Krivovichev and Brown (2001), bond parameters for W⁶⁺–O from Brese and O'Keeffe (1991), and bond parameters for Fe³⁺–O from Gagné and Hawthorne (2015).

but no detectable F, Cs and Rb. Therefore, only □, O, OH⁻, or H₂O is possible in the *Y* site of our sample.

The nature of the occupancy of the *Y* site was determined using the successful refinement procedure described by Li et al. (2020) for hydroxylplumbopyrochlore. (1) Omitting the O2 atom from the refinement results in *R*₁ = 0.051 and the largest peak in the difference-Fourier map shows 4.32 e⁻ at the *Y* site, suggesting an O[#] occupancy of >50%. (2) The site occupancy and displacement parameters for O2 were allowed to vary simultaneously, resulting in the site occupancy factor (s.o.f.) of O2 = 0.699 and *U*_{eq} = 0.087. This seems too high for this sample. If there are H atoms around the O2, the higher *U*_{eq} will contain part of the contributions of the H to the O2, leading to a higher s.o.f. value of the O2. (3) Based on the *U*_{eq} of the O2 fixed in a range of reasonable *U*_{iso} values, refinement results of the O2 occupancy were obtained as presented in Table 8. The *U*_{iso} value of 0.06 Å² in the *Y* site is acceptable in the structure refinement process of pyrochlore-supergroup minerals (Li et al., 2020), and it produces a good result of O_{0.62}□_{0.38}, with lower *R*₁ and *wR*₂ values than under the fully occupied model. (4) The difference-Fourier electron density (DFED) along (111) (Fig. 7) shows that there are obvious positive anomalies around O2 (in blue) compared to the lack of an obvious positive anomaly around O1 in the *X* site, which is powerful evidence of the existence of H atoms around O2 (Plasil et al., 2014). The 3D–DFED around O2 (Fig. 8) shows that ten maxima in the additional electron density occur, four of them directed towards the face centres and six towards edge mid-points of the [O2Pb₁₄] tetrahedron, away from the O2–Pb1 vectors; these are interpreted as possible locations of the H atoms. Angles between O–H vector directions

Table 5. Anisotropic displacement parameters and isotropic displacement parameters (Å²) for hydroplumboelsmoreite.

Atom	<i>U</i> ¹¹	<i>U</i> ²²	<i>U</i> ³³	<i>U</i> ¹²	<i>U</i> ¹³	<i>U</i> ²³	<i>U</i> _{eq}
Pb1(≡A)	0.0440(11)	0.0440(11)	0.0440(11)	-0.0040(6)	0.0035(6)	-0.0040(6)	0.0440(11)
W1(≡B)	0.0227(9)	0.0227(9)	0.0227(9)	0.0024(2)	0.0024(2)	-0.0024(2)	0.0227(9)
Fe1(≡B)	0.0227(9)	0.0227(9)	0.0227(9)	0.0024(2)	0.0024(2)	-0.0024(2)	0.0227(9)
O1(≡X)	0.028(6)	0.027(3)	0.027(3)	0.000	0.000	0.001(5)	0.027(2)
O2(≡Y)							0.060

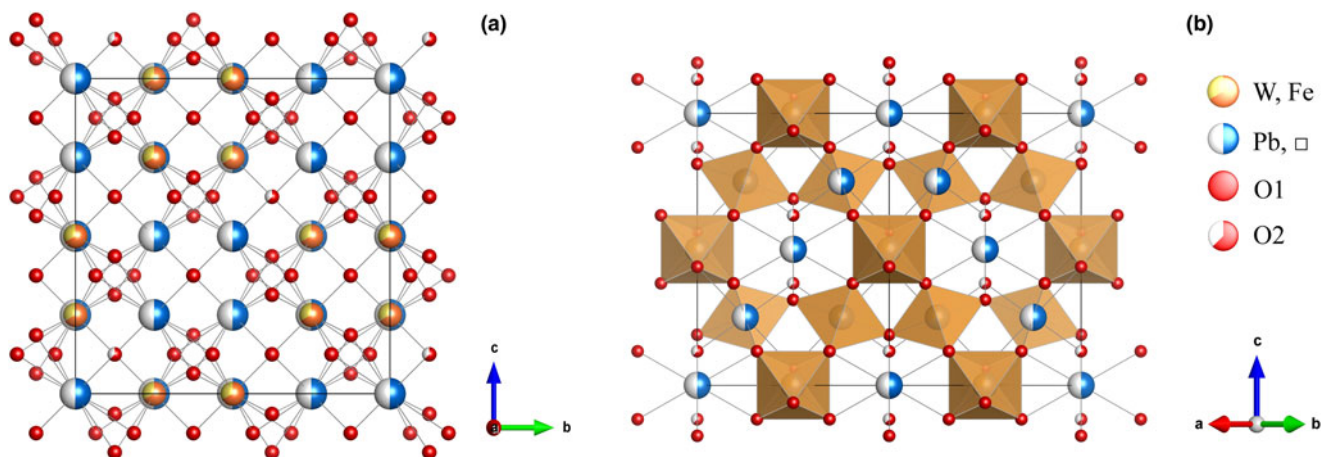


Fig. 6. General projection of the crystal structure of hydroplumboelsmoreite (a) along the a -axis and (b) the $[110]$ projection. A site: (Pb, \square). Drawn using *Vesta* (Momma and Izumi, 2011).

Table 8. Site occupancy factors (s.o.f), R_1 and difference-Fourier values for the Y site under different U_{iso} values.

	U_{eq}	R_1	wR_2	s.o.f.	Difference Fourier
O2 atom omitted		0.0514	0.1600	0	+4.32 e^-
Full s.o.f	0.14766	0.0464	0.1279	1	-0.24 e^-
Variable s.o.f and U_{iso}	0.08736	0.0456	0.1244	0.699	-0.52 e^-
Fixed U_{iso} 0.03	0.03	0.0467	0.1312	0.504	-1.01 e^-
Fixed U_{iso} 0.04	0.04	0.0465	0.1295	0.547	-0.88 e^-
Fixed U_{iso} 0.05	0.05	0.0461	0.1281	0.586	-0.77 e^-
Fixed U_{iso} 0.06	0.06	0.0459	0.1268	0.620	-0.69 e^-

such as $[111]^{\wedge}[1\bar{1}\bar{1}]$ and $[100]^{\wedge}[1\bar{1}\bar{1}]$ are 109.5° and 125.3° , respectively. These are broadly compatible with the 104° typical for an H_2O molecule and suggest possible orientations for that molecule. The Raman spectrum and BVS calculation also demonstrate

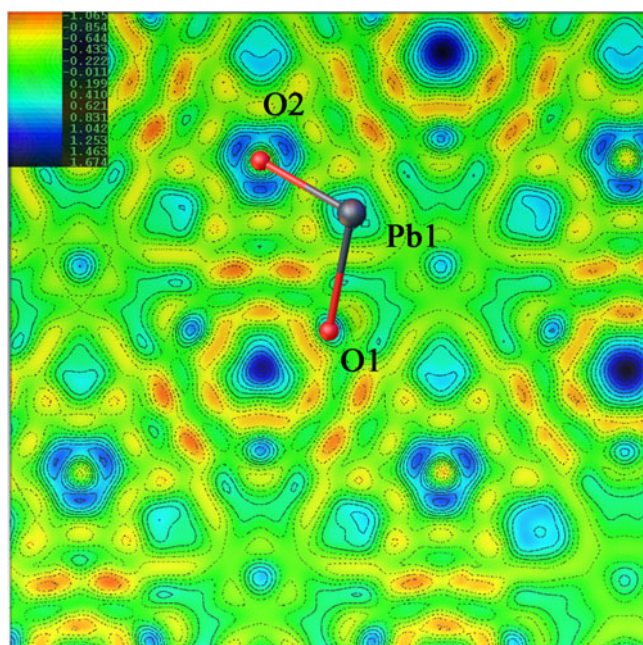


Fig. 7. Difference-Fourier electron density mapping along (111). Drawn using *Olex2* (Dolomanov *et al.*, 2009).

the existence of molecular H_2O in the Y site. As the determination of the exact H positions using only the DFED is not reliable, we do not list the atomic coordinates of H. (5) Subsequently, (${}^Y O_{0.62}^{\square} \square_{0.38}$) in the Y site is indicated, where O^{\square} denotes the amount of occupation needed to balance the formula's charge recalculated into O atoms. It should be noted that the empirical formula from the EMPA shows the requirement of a charge of -0.38 in the Y site, thus $0.43H_2O$, $0.19O^{2-}$ and $0.38\square$ (vacancy) are assigned to the Y site. This corresponds to the 1.27 wt.% H_2O chemical composition and 99.08 wt.% total. Therefore, the empirical formula calculated on the basis of $B=2$ is $(Pb_{1.05}Sr_{0.05}Ce_{0.07}Na_{0.01}\square_{0.82})_{\Sigma 2}(W_{1.32}Fe_{0.67}Zr_{0.01})_{\Sigma 2}O_6[(H_2O)_{0.43}O_{0.19}\square_{0.38}]_{\Sigma 1}$.

In fact, for the full or open occupancies of the Y site, or a fixed $U_{eq} = 0.06$, the refinements based on these three conditions lead to the Y site being occupied by $[(H_2O)_{0.81}O_{0.19}]$, $[(H_2O)_{0.51}O_{0.19}\square_{0.30}]$, or $[(H_2O)_{0.43}O_{0.19}\square_{0.38}]$, which all result in the conclusion that H_2O is dominant in the Y site.

Therefore, this new mineral is an elsmoreite-group mineral of the pyrochlore supergroup, and it was named hydroplumboelsmoreite according to the predominance of Pb in the A site and molecular H_2O in the Y site.

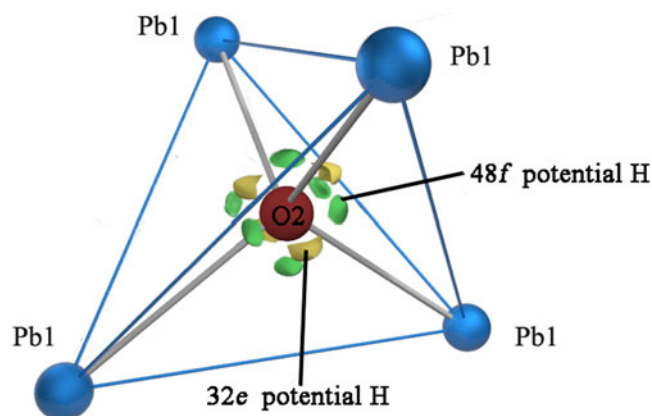


Fig. 8. Difference-Fourier electron density in the vicinity of the Pb1/O2 atoms. View of part of the hydroplumboelsmoreite structure, where the significant maxima of the positive difference electron density is located only around the O2 atom and four of them direct towards the face centres and six towards edge mid-points of the tetrahedron, away from the O2–Pb1 vectors.

Table 9. Comparison of the properties of the related elsmoreite-group minerals.*

Mineral species	Hydroplumboelsmoreite	'Hydroelsmoreite'	Hydrokenoelsmoreite-		Hydroxykenoelsmoreite
			3C	6R	
Simplified formula	$(\text{Pb}, \square)_2(\text{W}, \text{Fe}^{3+})_2\text{O}_6(\text{H}_2\text{O})$	$(\text{H}_2\text{O}, \text{Pb})_2(\text{W}, \text{Fe}^{3+})_2\text{O}_6(\text{H}_2\text{O})$	$(\square, \text{Na})_2(\text{W}, \text{Fe}^{3+}, \text{Al})_2(\text{O}, \text{OH})_6(\text{H}_2\text{O})$		$(\square, \text{Pb})_2(\text{W}, \text{Fe}^{3+}, \text{Al})_2(\text{O}, \text{OH})_6(\text{OH})$
Major component (wt.%)					
WO ₃	48.71	59.82	77.49	70.15	72.39
PbO	37.49	22.70	n.d.	n.d.	14.77
Al ₂ O ₃	0.01	0.02	2.41	0.97	1.67
Fe ₂ O ₃	8.50	6.75	5.83	8.17	5.99
Total (no H ₂ O)	97.81	93.34	88.68	82.68	95.01
H ₂ O	1.27 (calc.)	5.52 (calc.)	7.40 (calc.)	8.82 (calc.)	5.45 (calc.)
Total	99.08	98.86	96.08	90.85	100.46
Density (calc.)	7.47 g·cm ⁻³	6.78 g·cm ⁻³	6.025 g·cm ⁻³	6.025 g·cm ⁻³	5.806 g·cm ⁻³
Hardness					
– Mohs	4.5–5	3–4	±3	±3	~3
– Micro-indentation	278.59–302.3 kg·mm ⁻² (HV0.1kgf)	101.7–125.1 kg·mm ⁻² (HV0.1kgf)			
Unit cell parameters					
Crystal system, space group	cubic, <i>Fd</i> $\bar{3}m$	cubic, <i>Fd</i> $\bar{3}m$	cubic, <i>Fd</i> $\bar{3}m$	trigonal, <i>R</i> $\bar{3}$	trigonal, <i>R</i> $\bar{3}$
<i>a</i> (Å)	10.3377(5)	10.3421(5)	10.3065(3)	7.2882(2)	7.313(2)
<i>c</i> (Å)				35.7056(14)	17.863(7)
<i>V</i> (Å ³)	1104.77(16)	1106.18(17)	1094.80(6)	1642.51(9)	827(1)
<i>Z</i>	8	8	16	9	6
References	Our work	Our work	Mills et al. (2016); Williams et al. (2005)		Mills et al. (2017)
*Empirical formulae					
Hydroplumboelsmoreite	$(\text{Pb}_{1.05}\text{Sr}_{0.05}\text{Ce}_{0.07}\text{Na}_{0.01}\square_{0.82})_{\Sigma 2}(\text{W}_{1.32}\text{Fe}_{0.67}\text{Zr}_{0.01})_{\Sigma 2}\text{O}_6[(\text{H}_2\text{O})_{0.43}\text{O}_{0.19}\square_{0.38}]_{\Sigma 1}$				
'Hydroelsmoreite'	$[(\text{H}_2\text{O})_{0.76}\text{Pb}_{0.58}\text{Ce}_{0.06}\text{Sr}_{0.05}\text{Na}_{0.05}\text{Ca}_{0.04}\square_{0.46}]_{\Sigma 2}(\text{W}_{1.48}\text{Fe}_{0.49}\text{Al}_{0.02}\text{Zr}_{0.01})_{\Sigma 2}\text{O}_6(\text{H}_2\text{O}_{0.99}\text{O}_{0.01})_{\Sigma 1}$				
Hydrokenoelsmoreite-3C	$[\text{Na}_{0.28}\text{Ca}_{0.04}\text{K}_{0.02}(\text{H}_2\text{O})_{0.20}\square_{1.46}]_{\Sigma 2}(\text{W}_{1.47}\text{Fe}_{0.32}\text{Al}_{0.21}\text{As}_{0.01})_{\Sigma 2}(\text{O}_{4.79}(\text{OH})_{1.21})_{\Sigma 6}(\text{H}_2\text{O})$				
Hydrokenoelsmoreite-6R	$[\text{Na}_{0.24}\text{Ca}_{0.04}\text{K}_{0.03}(\text{H}_2\text{O})_{0.63}\square_{1.06}]_{\Sigma 2}(\text{W}_{1.42}\text{Fe}_{0.49}\text{Al}_{0.08}\text{As}_{0.01})_{\Sigma 2}[\text{O}_{4.65}(\text{OH})_{1.35}]_{\Sigma 6}(\text{H}_2\text{O})$				
Hydroxykenoelsmoreite	$(\square_{1.668}\text{Pb}_{0.315}\text{Ca}_{0.009}\text{Na}_{0.005}\text{K}_{0.003}\text{Ba}_{0.001})_{\Sigma 2}(\text{W}_{1.487}\text{Fe}_{0.357}\text{Al}_{0.156})_{\Sigma 2}[\text{O}_{4.119}(\text{OH})_{1.881}]_{\Sigma 6}(\text{OH})$				

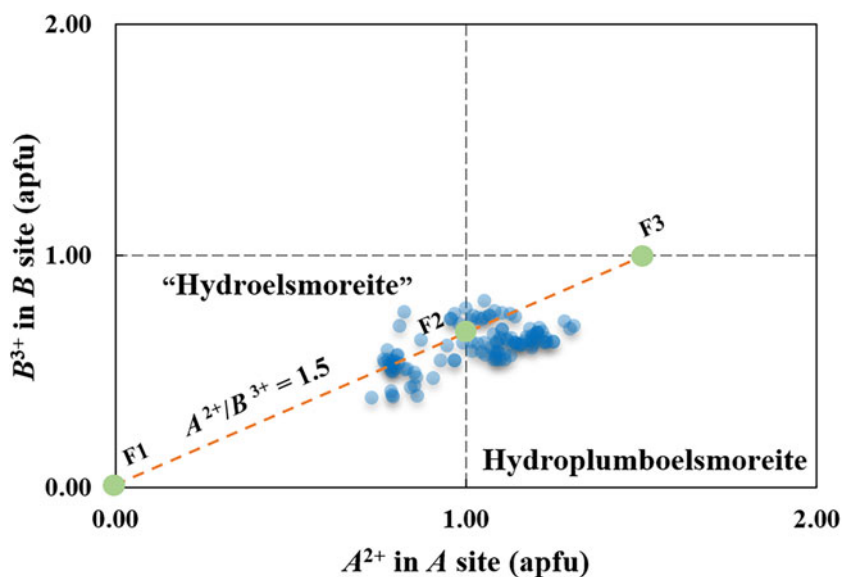


Fig. 9. Two-dimensional plots of the divalent *A* site cations and trivalent *B* site cations in hydroplumboelsmoreite and 'hydroelsmoreite'. F1 = $(A^0)_2W_2O_6(H_2O)$, F2 = $(PbA^0)_{\Sigma 2}(W_{1.33}Fe_{0.67}^{3+})_{\Sigma 2}O_6(H_2O)$, and F3 = $(Pb_{1.5}A^0_{0.5})_{\Sigma 2}(WFe^{3+})_{\Sigma 2}O_6(H_2O)$.

Discussion

Relationship to other mineral species

Hydroplumboelsmoreite is a new member of the pyrochlore supergroup. Its properties are compared with those of other members of the elsmoreite group in Table 9. A proposal for 'hydroelsmoreite' (IMA 2019-066) is being resubmitted to the CNMNC after revision. This phase is closely related to hydroplumboelsmoreite and was found in the same sample, but has obvious differences in chemical composition, crystal structure and hardness.

It should be noted that both of the previous two IMA-approved elsmoreite-group minerals, hydroxykenoelsmoreite (Mills *et al.*, 2016) and hydrokenoelsmoreite (Mills *et al.*, 2017), have been reported to deviate from the ideal cubic system due to ordering of Na and (\square, H_2O) in the *A* site or due to Fe^{3+} in the *B* site. However, the ordered distributions in these two sites were not observed in the hydroplumboelsmoreite analysed in this study and implies that the full cubic symmetry of the ideal pyrochlore structure is maintained. This phenomenon deserves more attention in elsmoreite-group minerals.

Chemical composition evolution

In the ideal formula, $(PbA^0)_{\Sigma 2}(W_{1.33}Fe_{0.67}^{3+})_{\Sigma 2}O_6(H_2O)$, which is charge balanced, the *A* site generally contains Pb^{2+} and other [8]-coordinated cations, and thus, the *B* site may contain subordinate Fe^{3+} or any other cations with lower charges to balance the charge. Neglecting minor substituents, the major components may have the following substitutions to make the formula electronically neutral: $(Pb_xA_{2-x}^0)_{\Sigma 2}(W_{2-y}Fe_y)_{\Sigma 2}O_6(H_2O)$. In addition, there is a proportionality between the bivalence cations in the *A* site and the trivalent cations in the *B* site, where $A^{2+}/B^{3+} = 1.5$ and $x = 1.5y$.

Thus, the electrically neutral end-member formula in the sense described by Hawthorne (2002) can be written as follows: if $y < 0.67$ and $x < 1$, the corresponding end-member formula is $(A^0)_2W_2O_6(H_2O)$ (labelled as F1 in Fig. 9), that is, 'hydroelsmoreite' or hydrokenoelsmoreite; otherwise, if $0.67 \leq y < 1$ and $1 \leq x \leq 2$, the corresponding end-member formula is $(PbA^0)_{\Sigma 2}(W_{1.33}Fe_{0.67}^{3+})_{\Sigma 2}O_6(H_2O)$ (labelled as F2 in Fig. 9) or

$(Pb_{1.5}A^0_{0.5})_{\Sigma 2}(WFe^{3+})_{\Sigma 2}O_6(H_2O)$ (labelled as F3 in Fig. 9), that is, hydroplumboelsmoreite. Hydroplumboelsmoreite and Pb-poor analogues such as 'hydroelsmoreite' and hydrokenoelsmoreite are named on the basis of dominant constituents of dominant valency groups in the *Y*, *A* and *B* sites in accord with Atencio *et al.* (2010). It should be noted that the end-member formula can be used as the ideal formula for hydroplumboelsmoreite is not unique although the former was found to be dominant in this study.

Making the assumption of negligible substitutions other than A^0 for Pb-dominant A^{2+} in the *A* site and Fe^{3+} for W^{6+} in the *B* site, 107 compositions obtained by WDS with polished fragments in the abovementioned epoxy block are plotted in Fig. 9. Although there is considerable solid solution that straddles the line between hydroplumboelsmoreite and 'hydroelsmoreite', the analysis points clearly cluster around the ideal composition F2 = $(PbA^0)_{\Sigma 2}(W_{1.33}Fe_{0.67}^{3+})_{\Sigma 2}O_6(H_2O)$.

Given the large charge difference between W and Fe, the preference for a W:Fe ratio of 2:1 may imply short-range order of these cations in the *B* site that is not reflected in the long-range average structure.

Conclusions

It appears that the original 'jixianite' sample with which the average chemical data (Liu, 1979) derived via wet-chemical analysis of powdered sample is a combination of raspite, hydroplumboelsmoreite and 'hydroelsmoreite'.

The compositional and crystal structural data collected in this study for a hydroplumboelsmoreite crystal unequivocally indicate that structurally, it belongs to the pyrochlore supergroup. Thus, it should be classified as hydroplumboelsmoreite in accordance with the classification rules for pyrochlore-supergroup minerals. It more specifically belongs to the elsmoreite group (W^{6+} predominantly in the *B* site), with Pb predominantly in the *A* site and H_2O predominantly in the *Y* site.

Acknowledgements. We acknowledge Prof. Ritsuro Miyawaki and Prof. Frédéric Hatert of the CNMNC and its members for their valuable suggestions on hydroplumboelsmoreite. A cotype specimen of 'jixianite' was provided by Liu Jianchang to whom we express our gratitude. We also thank Ge

Xiangkun and Tai Zongyao for their kind assistance of chemical analyses. In addition, we acknowledge the efforts of Principal Editor Stuart Mills and of reviewer Prof. Peter Leverett, Mike Rumsey and an anonymous reviewer for their detailed reviews. We appreciate all the authors of hydroxylplumbopyrochlore for their inspiration to us. This work was supported financially by the National Natural Science Foundation of China (41672043) and the China National Postdoctoral Program for Innovative Talents (BX20190304).

Supplementary material. To view supplementary material for this article, please visit <https://doi.org/10.1180/mgm.2021.86>

References

- Atencio D., Andrade M.B., Christy A.G., Giere R. and Kartashov P.M. (2010) The pyrochlore supergroup of minerals: nomenclature. *The Canadian Mineralogist*, **48**, 673–698.
- Brese N.E. and O’Keeffe M. (1991) Bond-valence parameters for solids. *Acta Crystallographica*, **B47**, 192–197.
- Brown I.D. (1977) Predicting bond lengths in inorganic crystals. *Acta Crystallographica*, **B33**, 1305–1310.
- Christy A.G. and Atencio D. (2013) Clarification of status of species in the pyrochlore supergroup. *Mineralogical Magazine*, **77**, 13–20.
- Dolomanov O.V., Bourhis L.J., Gildea R.J., Howard J.A.K. and Puschmann H. (2009) OLEX2: a complete structure solution, refinement and analysis program. *Journal of Applied Crystallography*, **42**, 339–341. <http://dx.doi.org/10.1107/S0021889808042726>.
- Farmer V.C. (1982) *The Infrared Spectra of Minerals*. Science Press, Beijing.
- Gadsden J.A. (1975) *Infrared Spectra of Minerals and Related Inorganic Compounds*. Butterworth, England, 152 pp.
- Gagne O.C. and Hawthorne F.C. (2015) Comprehensive derivation of bond-valence parameters for ion pairs involving oxygen. *Acta Crystallographica*, **B71**, 562–578.
- Gu Z.J., Ma Y., Zhai T.Y., Gao B.F., Yang W.S. and Yao J.N. (2006) A simple hydrothermal method for the large-scale synthesis of single crystal potassium tungsten bronze nanowires. *Chemistry A European Journal*, **12**, 7717–7723.
- Hawthorne F.C. (2002) The use of end-member charge-arrangements in defining new mineral species and heterovalent substitutions in complex minerals. *The Canadian Mineralogist*, **40**, 699–710.
- Jean L. and Bernard B. (2001) *Chekkcell*. Saint Martin, France.
- Krivovichev S.V. and Brown I.D. (2001) Are the compressive effects of encapsulation an artifact of the bond valence parameters? *Zeitschrift Fur Kristallographie*, **216**, 245–247.
- Li T., Li Z., Fan G., Fan H. and Nahdi M.M. (2020) Hydroxylplumbopyrochlore, $(\text{Pb}_{1.5}\square_{0.5})\text{Nb}_2\text{O}_6(\text{OH})$, a new member of the pyrochlore group from Jabal Sayid, Saudi Arabia. *Mineralogical Magazine*, **84**, 785–790.
- Liu J.C. (1979) Jixianite $\text{Pb}(\text{W},\text{Fe}^{3+})_2(\text{O},\text{OH})_7$ – A new tungsten mineral. *Acta Geologica Sinica*, **1**, 45–49.
- Mandarino J.A. (1981) The Gladstone-Dale relationship. IV. The compatibility concept and its application. *The Canadian Mineralogist*, **14**, 441–450.
- Mills S.J., Christy A.G., Rumsey M.S. and Spratt J. (2016) The crystal chemistry of elsmoreite from the Hemerdon (Drakelands) mine, UK: hydrokenoelsmoreite-3C and hydrokenoelsmoreite-6R. *Mineralogical Magazine*, **80**, 1195–1203.
- Mills S.J., Christy A.G., Kampf A.R., Birch W.D. and Kasatkin A. (2017) Hydroxykenoelsmoreite, the first new mineral from the Republic of Burundi. *European Journal of Mineralogy*, **29**, 491–497.
- Miyawaki R., Hatert F., Pasero M. and Mills S.J. (2021) CNMNC Newsletter 61. *Mineralogical Magazine*, **85**. <https://doi.org/10.1180/mgm.2021.48>.
- Momma K and Izumi F (2011) VESTA 3 for three-dimensional visualization of crystal, volumetric and morphology data. *Journal of Applied Crystallography*, **44**, 1272–1276.
- Pasero M. (2021) The New IMA List of Minerals. International Mineralogical Association. Commission on new minerals, nomenclature and classification (IMA-CNMNC). <http://cnmnc.main.jp/> [updated: January 2021].
- Plášil J., Škoda R., Fejfarová K., Čejka J., Kasatkin A.V., Dušek M., Talla D., Lapčák L., Machovič V. and Dini M. (2014) Hydroniumjarosite, $(\text{H}_3\text{O})^+\text{Fe}_2(\text{SO}_4)_2(\text{OH})_6$, from Cerros Pintados, Chile: Single-crystal X-ray diffraction and vibrational spectroscopic study. *Mineralogical Magazine*, **78**, 535–548.
- Sheldrick G.M. (2015) Crystal structure refinement with shelxl. *Acta Crystallographica*, **C71**, 3–8.
- Wang L.Y., Duo X.F., Tu L.P., Chen Y.L. and Wen X.M. (2013) Metallogenic law of tungsten deposit and the ore potential in Jixian Area, Tianjin. *Contributions to Geology and Mineral Resources Research*, **28**, 371–377.
- Warr L. (2021) IMA–CNMNC approved mineral symbols. *Mineralogical Magazine*, **85**, 291–320.
- Wen X.M., Zhu X.P., Zhang Q., Duo X.F. and Wang W.X. (2015) Research on metallogenic and geological characteristics of Panshan Granite Body in Jixian Country of Tianjin City. *Contributions to Geology and Mineral Resources Research*, **30**, 499–505.
- Williams P.A., Leverett P., Sharpe J.L., Colchester D.M. and Rankin J. (2005) Elsmoreite, cubic $\text{WO}_3 \cdot 0.5\text{H}_2\text{O}$, a new mineral species from Elsmore, New South Wales, Australia. *The Canadian Mineralogist*, **43**, 1061–1064.